An International Journal
JSCDSS
http://www.jscdss.com
Vol.7 No.1 February 2020: 7-12
Article history:
Accepted 30 November 2019
Published online 30 November 2019

Journal of Soft Computing and Decision Support Systems

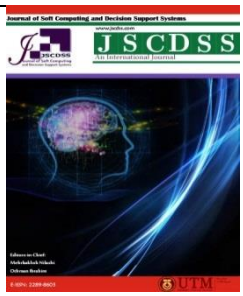

E-ISSN: 2289-8603

Anisotropic Diffusion-Based Unsharp Masking for Sharpness Improvement in Digital Images

Zohair Al-Ameen[a,*], Mayada A. Al-Healy [a], Rahma A. Hazim [a]
[a] Department of Computer Science, College of Computer Science and Mathematics, University of Mosul, Mosul, Nineveh, Iraq

*** Corresponding author email address**: qizohair@gmail.com

Abstract

Various available imaging systems are capturing images with deficient sharpness due to numerous unavoidable shortcomings. Perceiving and extracting information from such images is uneasy. Hence, it is required to process these images properly to produce sharper and clearer details. Many methods exist that can be used to increase the sharpness of digital images. Among such, the unsharp mask has gained high popularity due to its rapidness and simplicity. Still, this filter usually degrades the processed images by an overshoot effect, which appears around the edges as white shades. In this study, an anisotropic diffusion-based unsharp mask filter, so-called ADUSM, is proposed, in that the degraded image is filtered using an amended anisotropic diffusion filter rather than processing it only by a low-pass Gaussian filter. This modification permitted the attenuation of the overshoot artefact which yielded to obtain better quality results. The ADUSM is tested with several types of images and assessed with two adequate quality metrics. Many experiments indicated that the proposed filter can outperform different existing methods and produce satisfactory results with reasonable application time.

Keywords: Image sharpening, Anisotropic diffusion, Image enhancement, Unsharp mask.

1. Introduction

The acutance is an important feature in an image since the observer perceives properly if the image owns adequate edges and clear details. These two features are represented in an image by the information that has a high frequency. If such information is reduced or eliminated, the image apparent details will be tremendously degraded (Banham and Katsaggelos, 1997). Quite the opposite, improving such information can lead to noticeable visual improvements (Kim and Kwon, 2010). Image sharpening represents any method that can increase the visibility of edges and vital details of an unsharp image (Wilscy and Nair, 2008). Image sharpening is extensively utilized in recognition, printing, and photography to upsurge the acutance of digital images (Webb, 1989). There exist three key causes to increase the sharpness in an image which are, to highlight certain details, overcome the blurring effect introduced by the camera lens, and to upsurge legibility.

Hence, various methods are made available for image sharpening, wherein their intricacies vary according to the used concept. Such methods can be the use of morphological filtering (Schavemaker et al., 2000), APEX concept (Carasso, 2003), unsharp masking (Kim and Allebach, 2005), downscaling cokriging (Pardo-Igúzquiza et al., 2006), fuzzy bidirectional flow (Fu et al., 2007a), shock-diffusion equation (Fu et al., 2007b), sub-regions histogram equalization (Ibrahim and Kong, 2009), Sobolev gradient flows (Calder et al., 2010), fuzzy logic (Gui and Liu, 2011), Laplacian operators (Ma et al., 2014), Wavelets (Zafeiridis et al., 2016) and many more. As seen, different concepts are used for image sharpening. Among such, tremendous research has been made based on the unsharp mask concept in the past period due to its rapidness and simplicity. Still, it unavoidably degrades the processed image by the overshoot effect (Polesel et al., 2000). Such effect occurs around the edge sides, making these edges perceived with visible white shades (Cao et al., 2011). Thus, it is required to enhance the processing ability of the standard unsharp mask to provide artefact-free outcomes with better sharpness. Despite the major thrive in image sharpening, there still an adequate chance for ameliorating this filter. Therefore, an anisotropic diffusion-based unsharp mask filter, so-called ADUSM, is introduced in this study to provide enhanced sharpness for the processed images without delivering any unwanted effects.

In the proposed ADUSM, the image is processed by an amended anisotropic diffusion filter rather than processing it only by a low-pass Gaussian filter. This tactic provided an adequate chance in reducing the overshoot effect and facilitated the recovery of better-quality images. The developed ADUSM filter is tested with several types of

images, assessed with two adequate quality metrics and compared with three specialized sharpening methods.

The rest of this paper is structured as follows. The developed filter is presented in Section 2. The attained results and discussions are included in Section 3. Finally, the conclusion is provided in Section 4.

2. Proposed Filter

An ADUSM filter is introduced in this paper, in that it begins with the input of the degraded image and parameter λ, which controls the sharpness amount of the output image. Next, the amended anisotropic diffusion filter with 20 iterations is applied to attenuate the image components that have high frequencies. As the last step, the filter's output is passed to the unsharp masking filter to create the last output. In the upcoming subsections, adequate descriptions regarding the main steps of the ADUSM filter are delivered to provide a better understanding of the operation specifics of the proposed filter.

2.1 Anisotropic Diffusion Filter

This filter was first introduced in 1990 (Perona and Malik, 1990). Its main aim is to smooth an image without blurring it while keeping its important details. This filter starts by setting the required iterations number. Depending on intensive tests, good results were attained when the iterations number is set to 20. Next, the size of the image is determined so that, it can be used when calculating the four nearest-neighbour differences. At this point, the iterative process starts by computing the four nearest-neighbour differences using Eq. (1-4).

$$\nabla_N I_{i,j} = I_{i-1,j} - I_{i,j} \quad (1)$$

$$\nabla_S I_{i,j} = I_{i+1,j} - I_{i,j} \quad (2)$$

$$\nabla_E I_{i,j} = I_{i,j+1} - I_{i,j} \quad (3)$$

$$\nabla_W I_{i,j} = I_{i,j-1} - I_{i,j} \quad (4)$$

where $I_{i,j}$ is the smoothed image at each iteration, in which at the first iteration, it should fulfil $I_{i,j} = f_{i,j}$, where $f_{i,j}$ represents the input image. i,j are image coordinates; ∇_E, ∇_W, ∇_N, ∇_S represent the detected differences at the east, west, north, and south, respectively. The detected differences hold the high-frequency components of the image. Then, four conduction operators are calculated to attenuate the high-frequency components in each direction using Eq. (5-8).

$$g_N = \frac{1}{1 + \left(\frac{\nabla_N I_{i,j}}{K}\right)^2} \quad (5)$$

$$g_S = \frac{1}{1 + \left(\frac{\nabla_S I_{i,j}}{K}\right)^2} \quad (6)$$

$$g_E = \frac{1}{1 + \left(\frac{\nabla_E I_{i,j}}{K}\right)^2} \quad (7)$$

$$g_W = \frac{1}{1 + \left(\frac{\nabla_W I_{i,j}}{K}\right)^2} \quad (8)$$

where K is a scalar that controls the smoothness degree, in that K should satisfy ($K > 1$), as increasing the value of K produces a smoother output. The value of K is set to 7 in the standard anisotropic diffusion filter. In this study, parameter K is computed automatically based on local statistics using Eq. (9).

$$K = 2 * \left[\frac{mean(f_{i,j})}{\left(0.75 * \sigma(f_{i,j})\right)}\right] \quad (9)$$

where σ represents the standard deviation. Next, the entire image is smoothed using the divergence, which can be calculated using Eq. (10).

$$I_{i,j} = I_{i,j} + 0.25 * \begin{bmatrix} \left(g_N * \nabla_N I_{i,j}\right) + \left(g_S * \nabla_S I_{i,j}\right) + \\ \left(g_E * \nabla_E I_{i,j}\right) + \left(g_W * \nabla_W I_{i,j}\right) \end{bmatrix} \quad (10)$$

This process is repeated for 20 iterations as set earlier. After the end of the iterations, the output $I_{i,j}$ which is a smoothed image, is passed to the unsharp mask to compute the produce sharpened result.

2.2 Unsharp Mask (USM) Filter

It is a simple process that is used by various researchers to enhance the acutance of images presumed to have low sharpness. It improves the edges by subtracting an unsharp image from its original counterpart with the help of a scaling parameter. This filter is usually utilized in many areas related to photography to increase the apparent resolution of blurry images. The unsharp mask produces a sharp image using Eq. (11) (Kim and Allebach, 2005).

$$U_{i,j} = f_{i,j} + \lambda\left[f_{i,j} - G_{i,j}\right] \quad (11)$$

where, $f_{i,j}$ represents the pristine image; $U_{i,j}$ represents the sharpened image; λ represents a sharpening parameter which must satisfy ($\lambda > 0$), where a higher value provides a sharper result; $G_{i,j}$ represents image $f_{i,j}$ filter by a low-pass Gaussian filter; In this study, the output of the amended anisotropic diffusion filter is used within the USM filter as in Eq. (12).

$$Q_{i,j} = f_{i,j} + \lambda\left[f_{i,j} - I_{i,j}\right] \quad (12)$$

where, $Q_{i,j}$ represents the final outcome of the proposed filter. The result of the standard USM filter although looks better is a not precise depiction of the image's subject. Therefore, the proposed ADUSM filter is expected to provide better quality results than the standard USM in sharpening the details of different images. Finally, the outline of the developed filter is depicted in Fig. 1.

An International Journal JSCDSS E-ISSN: 2289-8603

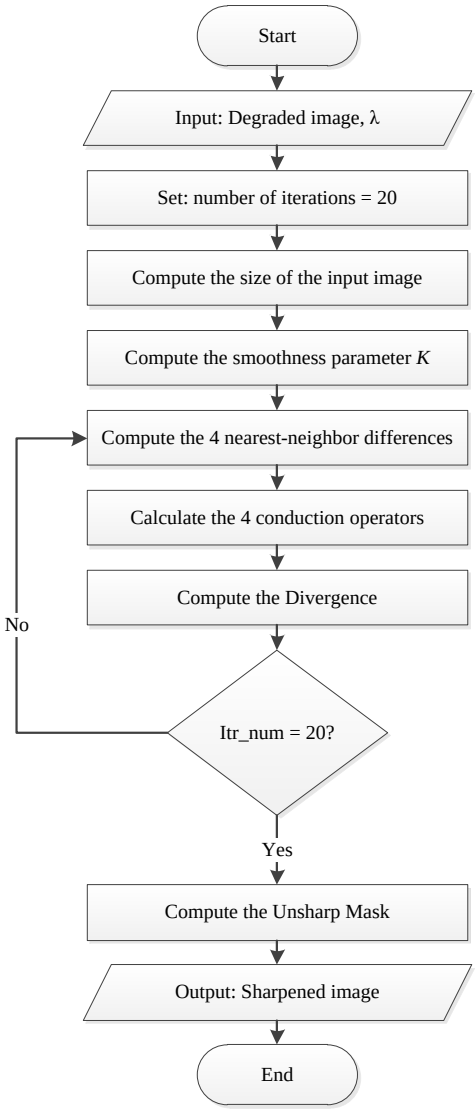

Fig. 1. The outline of the developed filter.

3. Results and Discussion

Here, the attained results, discussions and comparisons are stated. As for the utilized dataset, it contains various artificial and natural degraded images that are gathered from different online resources. As for the used image quality assessment (IQA) metrics, two of such were utilized namely discrete entropy (DE) (Toh and Isa, 2011) and just noticeable distortion based valid perception ratio (JND-VPR) (Zhan et al., 2017). Accordingly, the DE is considered as a no-reference metric that measures the accuracy depending on the contents of an image, and it describes the overall quality of a given image. Likewise, the JND-VPR is also a no-reference metric that evaluates a given image based on the local average brightness and local spatial frequency. This metric can be used to detect the existence of the overshoot effect around the edges. If the edges have a low local average brightness, it means that less overshoot effect occurs. The employed metrics provide a numeric value that describes the image quality, wherein higher values specify high perceived quality for DE and low perceived quality for JND-VPR and vice versa. Accordingly, the natural-degraded data are utilized in the conducted experiments while the artificial-degraded data are utilized in the conducted comparisons to reveal the real working ability of the developed filter. Regarding the comparable methods, the ADUSM filter is benchmarked with the Laplacian filter (LF), (Yang, 2014), traditional shock filter (TSF) (Osher and Rudin, 1990), traditional unsharp mask filter (TUSM) (Panetta et al., 2011) and amended unsharp mask filter (AUSM) (Al-Ameen et al., 2019). The computer specifics that are utilized to conduct this study are a 2.8 core I7 CPU and 16 GB of memory, while the programming language used to develop this filter is MATLAB 2018a.

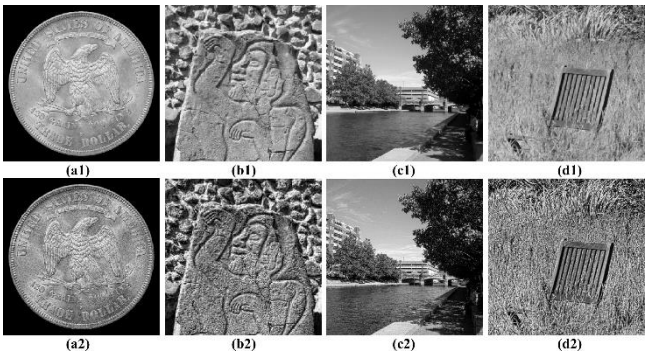

Fig. 2. The results of ADUSM on real-degraded grayscale images for (a1-d1) real-blurred images and (a2-d2) the resulting images from applying ADUSM with λ = (2, 1.5, 2.3, and 1.4).

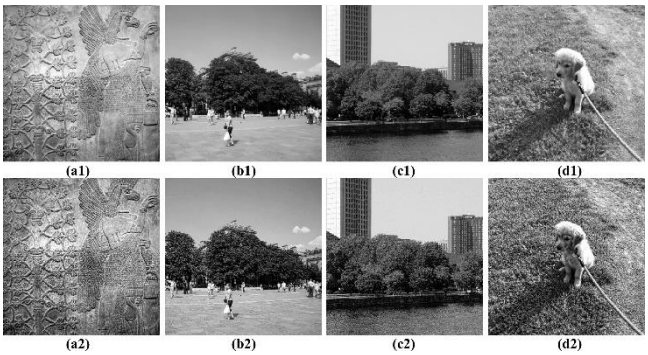

Fig. 3. The results of ADUSM on real-degraded grayscale images for (a1-d1) real-blurred images and (a2-d2) the resulting images from applying ADUSM with λ = (1.3, 2.2, 2.4, and 1.3).

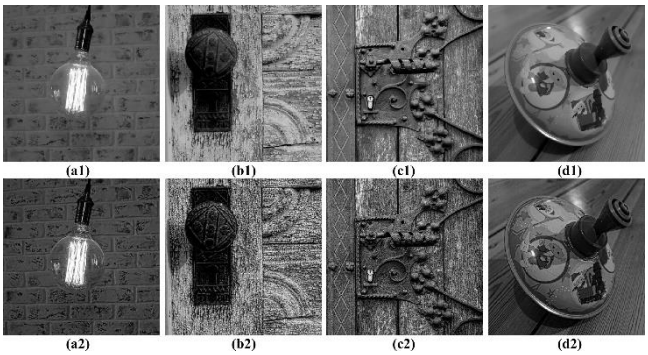

Fig. 4. The results of ADUSM on real-degraded grayscale images for (a1-d1) real-blurred images and (a2-d2) the resulting images from applying ADUSM with λ = (2.1, 2.7, 2.5, and 3).

An International Journal JSCDSS E-ISSN: 2289-8603

Fig. 2 – Fig. 4 show the attained experimental outcomes using ADUSM. Fig. 5 – Fig. 7 display the outcomes of the attained comparisons. Table 1 exhibits the scores of the used metrics for the achieved comparisons. Fig. 8 demonstrates the graphical charts of the mean readings in Tables 1. Using the outcomes displayed in Fig.2 – Fig. 4, the ADUSM delivered results with adequate quality without an obvious introduction to the overshoot artefact. In addition, the outcomes of ADUSM have satisfactory details, seemed natural, and have very much alike illumination to the original images. As seen from the results of comparisons in Table 1 and Fig. 5 – Fig. 8, it is evident that the ADUSM filter achieved the best IQA scores since it delivered outcomes with high sharpness without generating any visible overshoot effect or visual flaws with a moderate runtime.

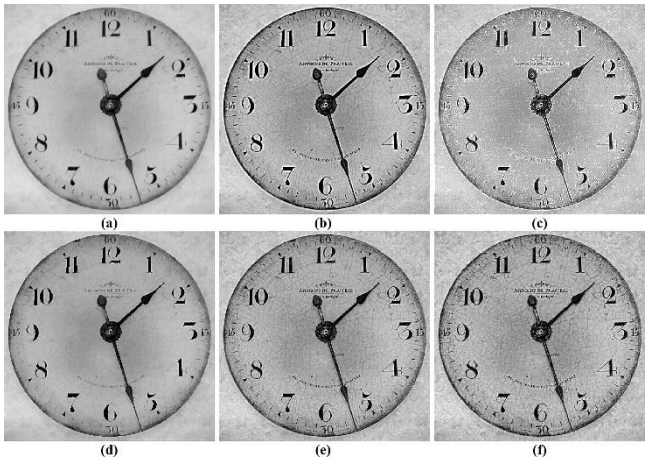

Fig. 5. The outcome of the conducted comparison between ADUSM and the other comparative methods. (a) blurry image; the other images are filtered by: (b) TSUM; (c) LF; (d) TSF; (e) AUSM; (f) ADUSM.

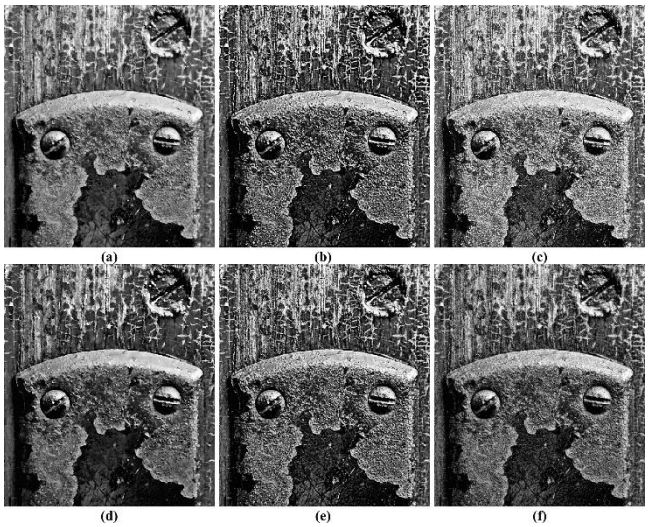

Fig. 6. The outcome of the conducted comparison between ADUSM and the other comparative methods. (a) blurry image; the other images are filtered by: (b) TSUM; (c) LF; (d) TSF; (e) AUSM; (f) ADUSM.

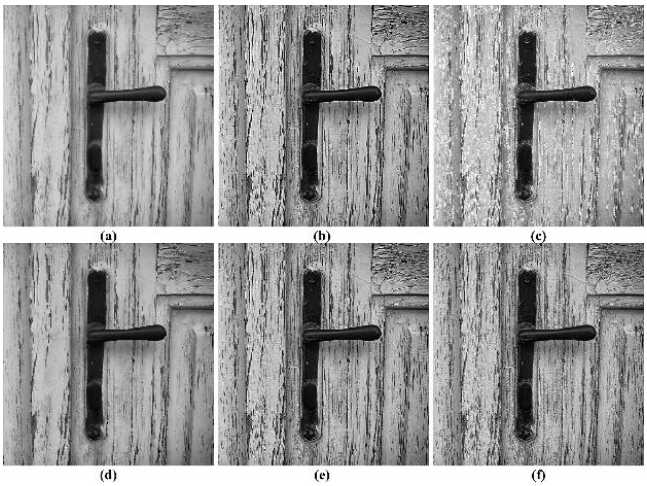

Fig. 7. The outcome of the conducted comparison between ADUSM and the other comparative methods. (a) blurry image; the other images are filtered by: (b) TSUM; (c) LF; (d) TSF; (e) AUSM; (f) ADUSM.

Table 1
The IQA scores and the recorded runtimes for the made comparisons.

Comparatives	Figure	DE	JND-VPR	Time
Degraded	8	6.7215	0.3195	-
	9	7.7043	0.2920	-
	10	7.2935	0.2828	-
	Average	7.2397	0.2981	-
TUSM	8	6.9995	0.4159	0.057918
	9	7.2743	0.4187	0.062186
	10	7.7061	0.4136	0.064715
	Average	7.3266	0.4160	**0.061600**
LF	8	7.1013	0.4859	0.129769
	9	7.5500	0.5224	0.053760
	10	7.5816	0.5091	0.050049
	Average	7.4109	0.5058	0.077800
TSF	8	6.7218	0.7118	0.321410
	9	7.7181	0.5568	0.604097
	10	7.3296	0.6368	0.685928
	Average	7.2565	0.6351	0.645000
AUSM	8	6.9654	0.3711	0.978581
	9	7.5260	0.3856	2.172914
	10	7.6839	0.3960	2.549688
	Average	7.3917	0.3842	1.900300
Proposed ADUSM	8	7.0502	0.2761	0.138039
	9	7.7258	0.2460	0.267222
	10	7.7126	0.3063	0.327828
	Average	**7.4962**	**0.2761**	0.244363

As for the TSUM, it presented the overshoot effect, that is why it did not score well in terms of IQA. However, it was the fastest technique. As for the Laplacian filter, it scored well in with DE yet somewhat low in JND-VPR due to the high presentation of the overshoot effect. Still, it provided a quite fast runtime. As for the traditional shock filter, it delivered adequately sharpened edges in its outcomes. However, it provided two drawbacks. The first being the generation of the undesirable staircase artefact to the results. This effect reduces the visible quality making the resulting images appear different than their original versions. The second being the deliveries of slow runtime.

An International Journal JSCDSS E-ISSN: 2289-8603

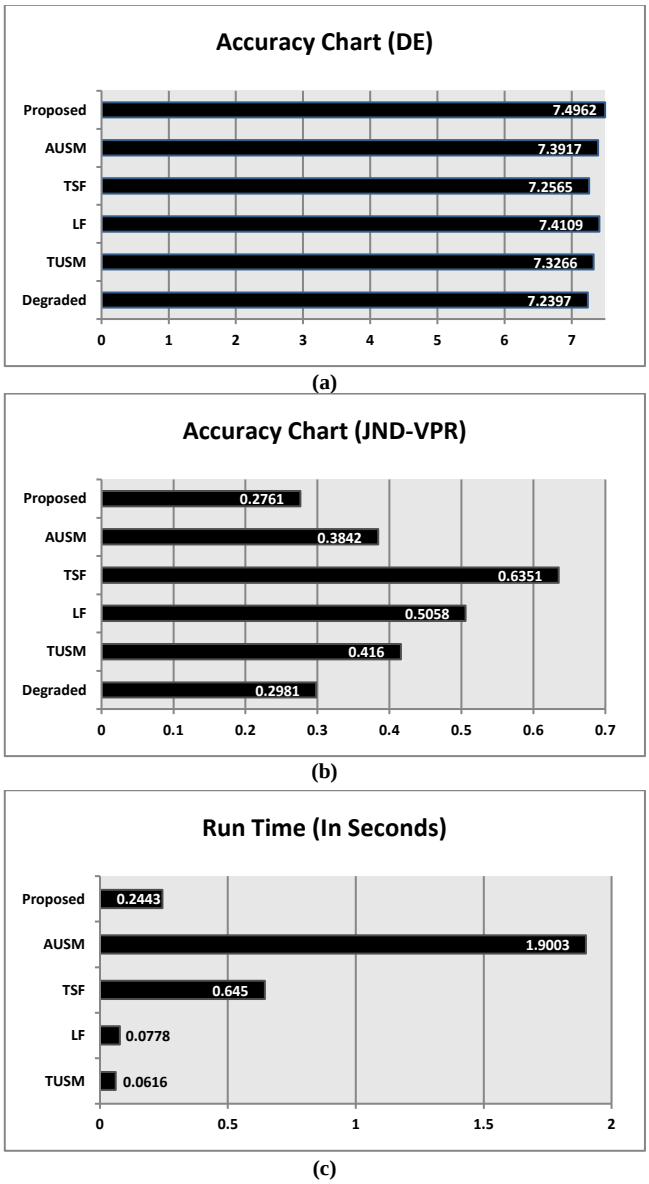

Fig. 8. The graphical charts of the mean readings in Tables 1 for (a) DE, (b) JND-VPR and (c) Runtime.

As for the AUSM, it was very competitive to the proposed filter in terms of IQA scores as it achieved well in the used assessment metrics. However, it was the slowest among the compared techniques. Improving the performance of a standard method to produce acceptable results is an uneasy task, yet it has evidently done in this study since the developed ADUSM filter provided results with natural contrast, proper brightness, and no visual flaws. This is significant because such achievement is made possible with low-complexity modifications. To end with, the proposed filter is anticipated to be used for many existing real-life applications.

4. Conclusion

In this paper, a low-intricacy ADUSM is developed to enhance the acutance of digital images. It utilizes an amended anisotropic diffusion filter to process the image rather than utilizing the low-pass Gaussian filter. This modification permitted the attenuation of the overshoot artefact which yielded to obtain better quality details. The ADUSM is compared with four specialized techniques and tested using natural-degraded images. Moreover, the attained results are assessed via two adequate methods of DE and JND-VPR. The attained results revealed that the ADUSM delivered adequate outcomes and outperformed certain comparison techniques, wherein it scored the best in quality metrics. Accordingly, the ADUSM delivered results with adequate quality without an obvious introduction to the overshoot artefact. In addition, the outcomes of ADUSM have satisfactory details, seemed natural, and have very much alike illumination to the original images. As the last point, utilizing simple filters to increase the acutance is required in various imaging schemes with low hardware specs.

References

Al-Ameen, Z., Muttar, A., & Al-Badrani, G. (2019). Improving the Sharpness of Digital Image Using an Amended Unsharp Mask Filter. *International Journal of Image, Graphics and Signal Processing*, *11*(3), 1-9.

Banham, M. R., & Katsaggelos, A. K. (1997). Digital image restoration. *IEEE signal processing magazine*, *14*(2), 24-41.

Calder, J., Mansouri, A., & Yezzi, A. (2010). Image sharpening via Sobolev gradient flows. *SIAM Journal on Imaging Sciences*, *3*(4), 981-1014.

Cao, G., Zhao, Y., Ni, R., & Kot, A. C. (2011). Unsharp masking sharpening detection via overshoot artifacts analysis. *IEEE Signal Processing Letters*, *18*(10), 603-606.

Carasso, A. S. (2003). The APEX method in image sharpening and the use of low exponent Lévy stable laws. *SIAM Journal on Applied Mathematics*, *63*(2), 593-618.

Fu, S. J., Ruan, Q. Q., & Wang, W. Q. (2007b). A shock-diffusion equation with local coupling term for image sharpening. *Journal of Optoelectronics Laser*, *18*(2), 245-253.

Fu, S., Ruan, Q., Wang, W., Gao, F., & Cheng, H. D. (2007a). A feature-dependent fuzzy bidirectional flow for adaptive image sharpening. *Neurocomputing*, *70*(4-6), 883-895.

Gui, Z., & Liu, Y. (2011). An image sharpening algorithm based on fuzzy logic. *Optik-International Journal for Light and Electron Optics*, *122*(8), 697-702.

Ibrahim, H., & Kong, N. S. P. (2009). Image sharpening using sub-regions histogram equalization. *IEEE Transactions on Consumer Electronics*, *55*(2), 891- 895.

Kim, K. I., & Kwon, Y. (2010). Single-image super-resolution using sparse regression and natural image prior. *IEEE transactions on pattern analysis and machine intelligence*, *32*(6), 1127-1133.

Kim, S. H., & Allebach, J. P. (2005). Optimal unsharp mask for image sharpening and noise removal. *Journal of Electronic Imaging*, *14*(2), 023005-1- 023005-13.

Kim, S. H., & Allebach, J. P. (2005). Optimal unsharp mask for image sharpening and noise removal. *Journal of Electronic Imaging*, *14*(2), 023005-1-023005-13.

Ma, T., Li, L., Ji, S., Wang, X., Tian, Y., Al-Dhelaan, A., & Al-Rodhaan, M. (2014). Optimized Laplacian image sharpening algorithm based on graphic processing unit. *Physica A: Statistical Mechanics and its Applications*, *416*, 400-410.

Osher, S., & Rudin, L. I. (1990). Feature-oriented image enhancement using shock filters. *SIAM Journal on numerical analysis*, *27*(4), 919-940.

An International Journal JSCDSS E-ISSN: 2289-8603

Panetta, K., Zhou, Y., Agaian, S., & Jia, H. (2011). Nonlinear unsharp masking for mammogram enhancement. *IEEE Transactions on Information Technology in Biomedicine*, *15*(6), 918-928.

Pardo-Igúzquiza, E., Chica-Olmo, M., & Atkinson, P. M. (2006). Downscaling cokriging for image sharpening. *Remote Sensing of Environment*, *102*(1-2), 86-98.

Perona, P., & Malik, J. (1990). Scale-space and edge detection using anisotropic diffusion. *IEEE Transactions on pattern analysis and machine intelligence*, *12*(7), 629-639.

Polesel, A., Ramponi, G., & Mathews, V. J. (2000). Image enhancement via adaptive unsharp masking. *IEEE transactions on image processing*, *9*(3), 505-510.

Schavemaker, J. G., Reinders, M. J., Gerbrands, J. J., & Backer, E. (2000). Image sharpening by morphological filtering. *Pattern Recognition*, *33*(6), 997-1012.

Toh, K., & Isa, N. (2011). Locally adaptive bilateral clustering for image deblurring and sharpness enhancement. *IEEE Transactions on Consumer Electronics*, *57*(3), 1227-1235.

Webb, G. (1989). Sharpness issues in colour printing. *The Journal of Photographic Science*, *38*(4-5), 173-176.

Wilscy, M., & Nair, M. S. (2008, June). A new method for sharpening color images using fuzzy approach. In *International Conference Image Analysis and Recognition* (pp. 65-74). Springer, Berlin, Heidelberg.

Yang, C. C. (2014). Finest image sharpening by use of the modified mask filter dealing with highest spatial frequencies. *Optik-International Journal for Light and Electron Optics*, *125*(8), 1942-1944.

Zafeiridis, P., Papamarkos, N., Goumas, S., & Seimenis, I. (2016). A New Sharpening Technique for Medical Images using Wavelets and Image Fusion. *Journal of Engineering Science & Technology Review*, *9*(3), 187–200.

Zhan, K., Shi, J., Teng, J., Li, Q., Wang, M., & Lu, F. (2017). Linking synaptic computation for image enhancement. *Neurocomputing*, *238*, 1-12.

An International Journal
JSCDSS
E-ISSN: 2289-8603